B and D meson Suppression and Azimuthal Anisotropy in a Strongly Coupled Plasma at $\sqrt{s_{NN}} = 5.5$ TeV

Blessed Arthur Ngwenya
(ngwble001@myuct.ac.za)
W. A. Horowitz

University of Cape Town (South Africa)
arXiv:2011.07617

26-31 Mar, 2023 (Hard Probes 2023)

Introduction

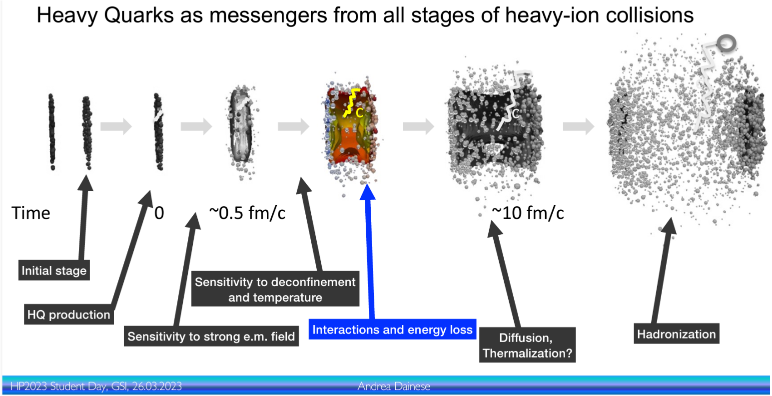

- Model energy loss of HQ propagating through QGP
- Large m (early production, scale separation)
- Strong coupling ($\eta/s \sim 0.1$) and transport coefficients

Some Lessons from Experiments

- Experimental results simultaneously suggest:
  1. strongly coupled plasma that evolves hydrodynamically with coupling, $\alpha \gtrsim 1$ from low p_T observables (low T)
     - AdS/CFT, LQCD
  2. weakly coupled gas of slightly modified quarks and gluons with coupling, $\alpha < 1$ (high T)
     - pQCD

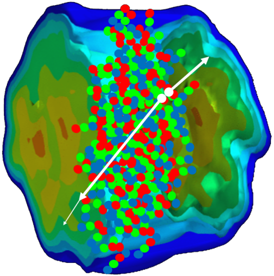

Langevin Energy Loss

$$\frac{dp_i}{dt} = -\mu p_i + F_i^L + F_i^T \quad (1)$$

$$\mu = \frac{\pi\sqrt{\lambda}T^2}{2M_Q} \quad (2)$$

$$< F_i^L(t_1)F_j^L(t_2) > = \kappa_L \hat{p}_i \hat{p}_j g(t_2 - t_1) \quad (3)$$

$$< F_i^T(t_1)F_j^T(t_2) > = \kappa_T(\delta_{ij} - \hat{p}_i \hat{p}_j) g(t_2 - t_1) \quad (4)$$

$$\kappa_T = \pi\sqrt{\lambda}T^3\gamma^{1/2}, \quad \kappa_L = \gamma^2\kappa_T \quad (5)$$

$$\gamma \lesssim \gamma_{crit}^{fluc} = \frac{M_Q^2}{4T^2} \quad (6)$$

Parameter mapping between QCD and $\mathcal{N} = 4$ SYM

- **Equal Temperature and Parameters (ET):**
  - $T_{QCD-plasma} = T_{SYM-plasma}$ and $\lambda = 4\pi\alpha_s N_c = 4\pi \times 0.3 \times 3$
- **Equal Energy Density and HQ Potential (EE):**
  - $T_{SYM-plasma} = T_{QCD-plasma}/3^{1/4}$ and $\lambda = 5.5$
- Uncertainties associated with diffusion coefficient in AdS/CFT
  - D(p), but longitudinal fluctuations grow as $\gamma^{5/2}$
  - D=const
- We've explored four combinations of these setups

B-meson $\mathbf{R_{AA}(p_T)}$ Data Comparison at $\sqrt{s_{NN}} = \mathbf{2.76}$ TeV

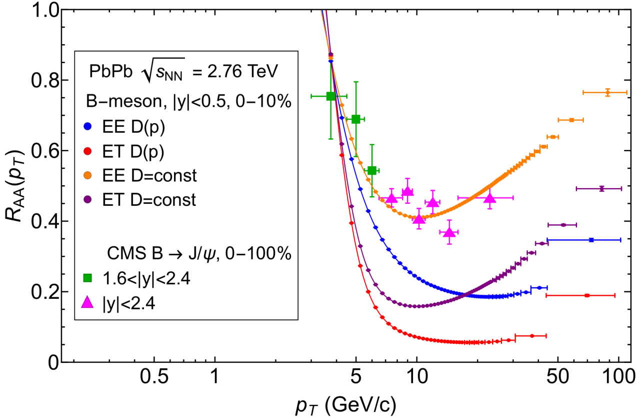

Figure 1: B meson $R_{AA}(p_T)$ qualitative comparison to CMS measurements at $\sqrt{s_{NN}} = 2.76$ TeV

$R_{AA}(p_T)$ Centrality Dependence at $\sqrt{s_{NN}} = 5.5$ TeV

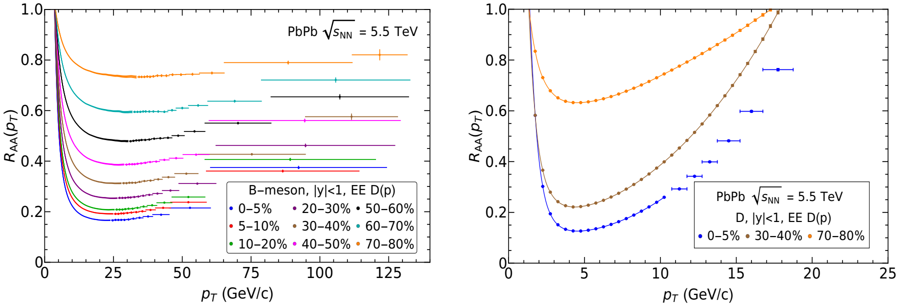

(a) B mesons (b) D mesons

Figure 2: EE, $D(p)$ $R_{AA}(p_T)$ at $\sqrt{s_{NN}} = 5.5$ TeV for centrality classes 0-5% up to 70-80%.

$R_{AA}(p_T)$ for various setups

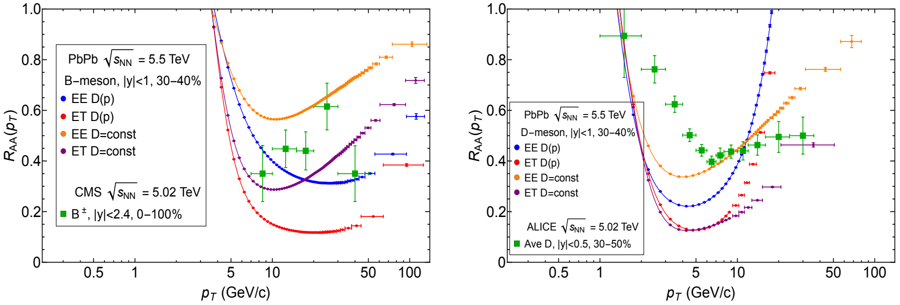

(a) B mesons (b) D mesons

Figure 3: B and D-meson $R_{AA}(p_T)$ for various parameters at $\sqrt{s_{NN}} = 5.5$ TeV for the 30-40% centrality class.

Key observations from $R_{AA}(p_T)$ results

- EE, D=const $R_{AA}(p_T)$ results are qualitatively consistent with CMS data at $\sqrt{s_{NN}} = 2.76$ TeV
- Suppression decreases with centrality
- The $R_{AA}(p_T)$ $D(p)$ setup has less suppression compared to $D = const$ due to fluctuations
- The $R_{AA}(p_T)$ $D(p)$ setup breaks down at high momentum (unreliable for D-mesons)
- In the $D = const$ setup, $\mu \sim 1/E$ (fluctuation dissipation theorem), so drag is smaller at high-p_T, implying less suppression
- There's less suppression in the EE setup compared to ET due to a smaller drag

$\mathbf{v_2(p_T)}$ Data Comparison at $\sqrt{s_{NN}} = 2.76$ TeV

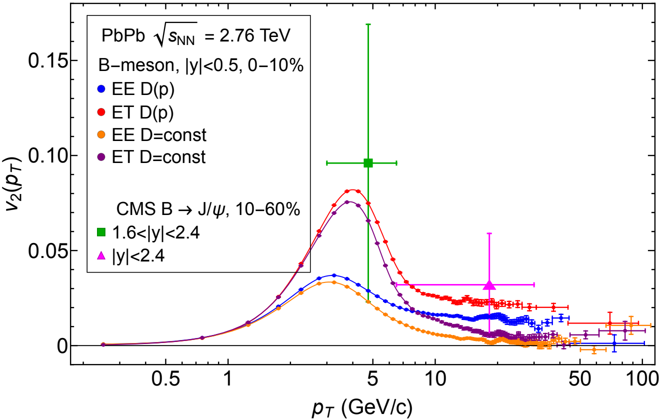

Figure 4: B meson $v_2(p_T)$ qualitative comparison to CMS measurements at $\sqrt{s_{NN}} = 2.76$ TeV

$\mathbf{v_2(p_T)}$ Centrality Dependence at $\sqrt{s_{NN}} = \mathbf{5.5}$ TeV

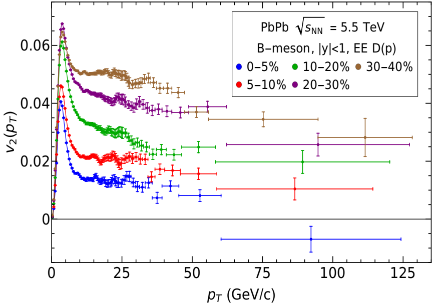

(a) B mesons

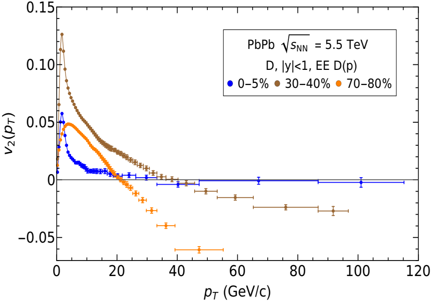

(b) D mesons

Figure 5: EE, $D(p)$ $v_2(p_T)$ at $\sqrt{s_{NN}} = 5.5$ TeV for various centrality classes.

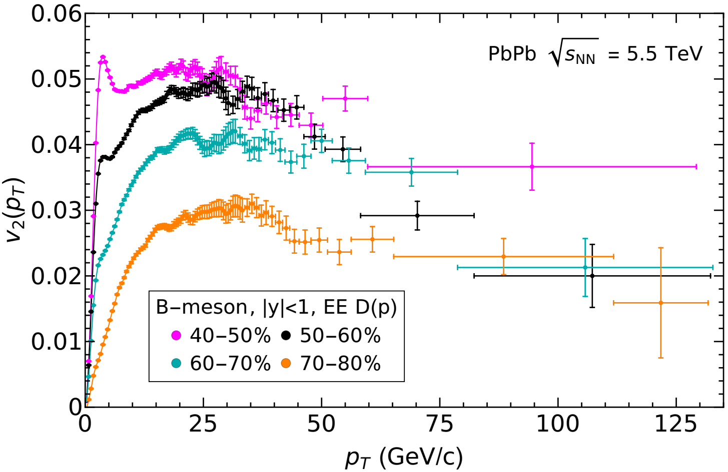

Figure 6: *EE*, $D(p)$ B-meson $v_2(p_T)$ at $\sqrt{s_{NN}} = 5.5$ TeV for the centrality classes 40-50% up to 70-80%.

$\mathbf{v_2(p_T)}$ for various setups

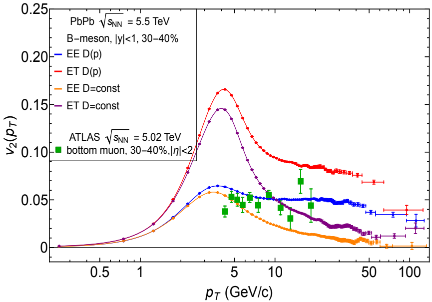

(a) B mesons

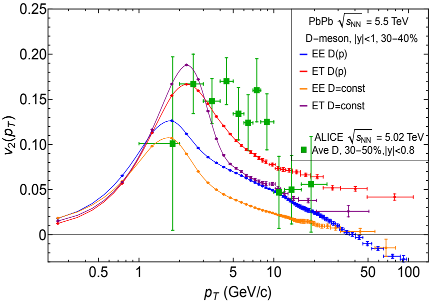

(b) D mesons

Figure 7: B and D-meson $v_2(p_T)$ at $\sqrt{s_{NN}} = 5.5$ TeV for the 30-40% centrality class.

Key observations from $v_2(p_T)$ results

- EE, D=const consistent with CMS B $R_{AA}(p_T)$ at $\sqrt{s_{NN}} = 2.76$ TeV shows largest tension with B $v_2(p_T)$
- $v_2(p_T)$ increases with centrality up to $30 - 40\%$ centrality then decreases
- The peak in $v_2(p_T)$ occurs at $p_T \sim M_Q$
- Anti-correlation between $R_{AA}(p_T)$ and $v_2(p_T)$, more suppression means quarks are more sensitive to the medium
- At high-p_T, $v_2(p_T)$ decreases as the $R_{AA}(p_T)$ increases

Decoupling Energy Loss and Flow: B mesons

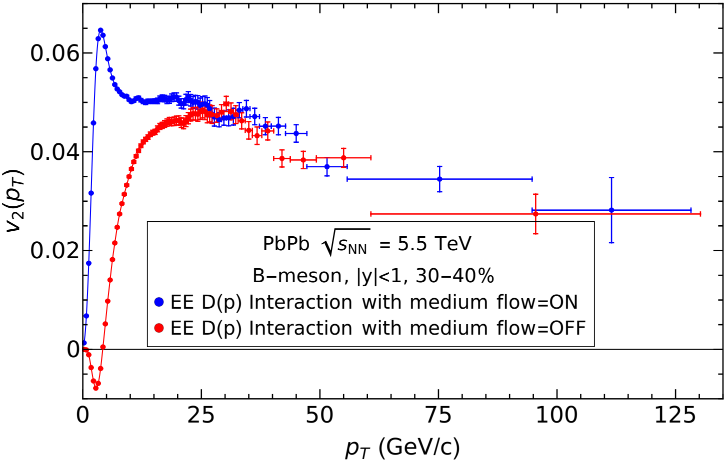

Figure 8: B-meson $v_2(p_T)$ at $\sqrt{s_{NN}} = 5.5$ TeV for the 30-40% centrality class when the interaction with the medium flow is on compared to when the interaction is off.

Decoupling Energy Loss and Flow: D mesons

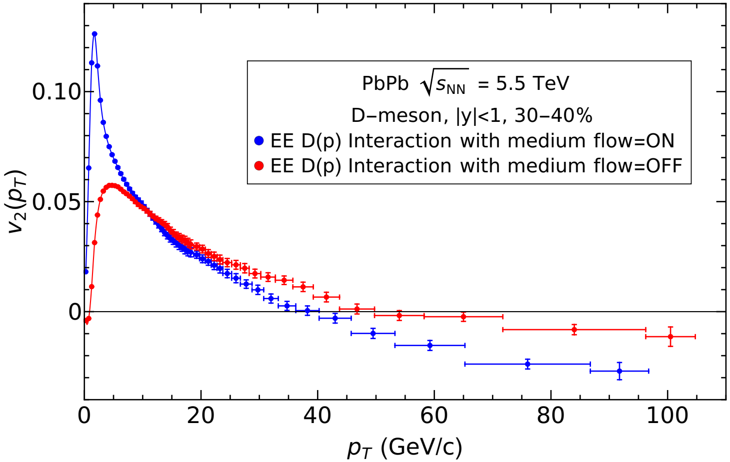

Figure 9: D-meson $v_2(p_T)$ at $\sqrt{s_{NN}} = 5.5$ TeV for the 30-40% centrality class when the interaction with the medium flow is on compared to when the interaction is off.

Summary

- Computed heavy quark energy loss assuming strong coupling
- Various AdS/CFT parameters employed to account for uncertainties
- B, D-meson $R_{AA}(p_T)$ and $v_2(p_T)$ predictions at $\sqrt{s_{NN}} = 5.5$ TeV
- Qualitative comparison with data from various LHC experiments
- Decoupling energy loss from medium flow

Outlook

- Provide further predictions for D-mesons
- Quantitative comparison of these predictions to LHC-Run 3 data
- Study other collision systems i.e. $Xe + Xe$, pPb
- AdS/CFT energy loss calculations in low energy heavy-ion collisions

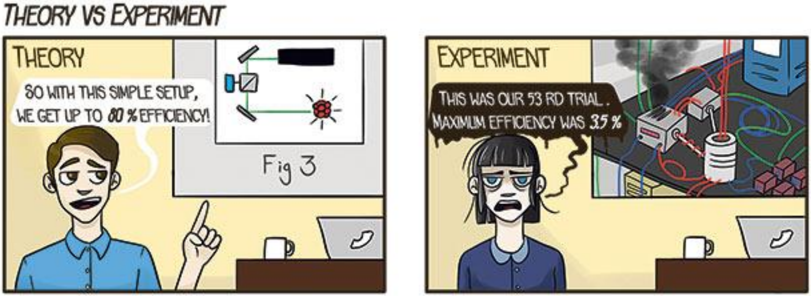

Thank you for your attention!
Danke!

Questions? Comments?

Did you hear the joke about covid-19?

Never mind, I don't want to spread it around!

Production Geometry using the Glauber Model

$$\rho(r) = \rho_0 \frac{1 + w\,(r/R)^2}{1 + exp\left(\frac{r-R}{a}\right)} \tag{7}$$

$$n_{BC}(x, y; b) = AB\sigma_{inel}^{NN} T_A\left(x - \frac{b}{2}, y\right) T_B\left(x + \frac{b}{2}, y\right) \tag{8}$$

- R is the nuclear radius, a is the skin depth and w characterizes deviations from a spherical shape
- Provides a quantitative way to simulate geometrical configuration of the nuclei when they collide
- Computation of geometrical quantities i.e number of colliding/participating nucleons

Centrality classes for heavy quark production

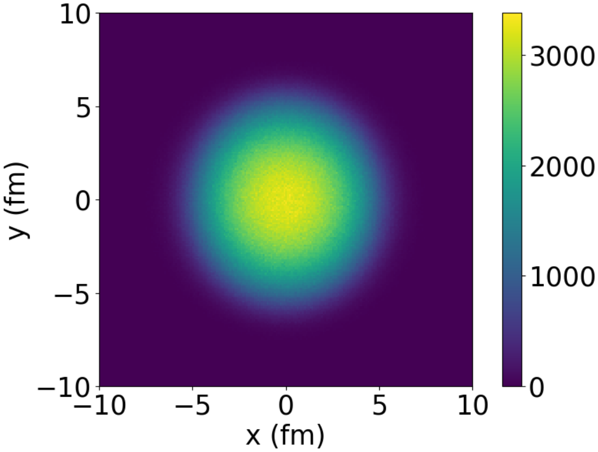

Figure 10: Unnormalised binned 2D collision density for the Pb+Pb 0-5% centrality class at $\sqrt{s} = 5.5$ TeV with a total of 20 million heavy quarks.

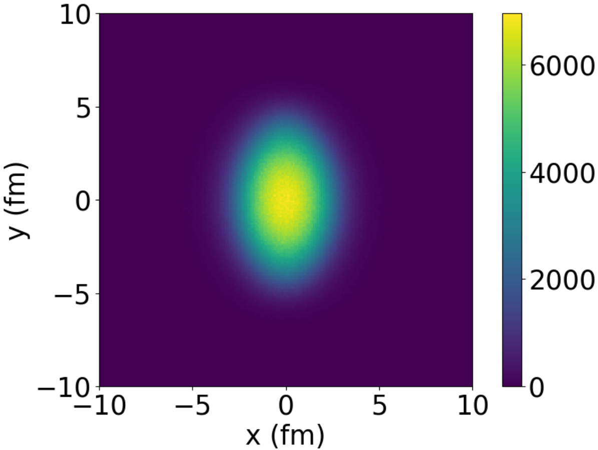

Figure 11: Unnormalised binned 2D collision density for the Pb+Pb 20-30% centrality class at $\sqrt{s} = 5.5$ TeV with a total of 20 million heavy quarks.

Cross sections of MC random numbers

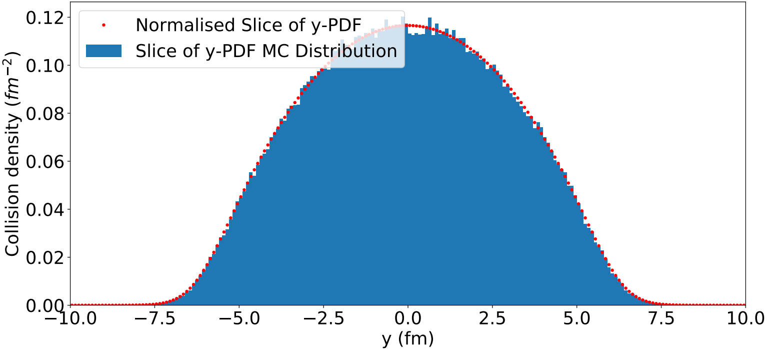

Figure 12: Cross section (along y) of the binned 2D collision density at $x = 0.05$ fm for the $Pb + Pb$ 0-5% centrality class at $\sqrt{s_{NN}} = 5.5$ TeV. The histogram shows Monte Carlo generated random numbers obeying this distribution.

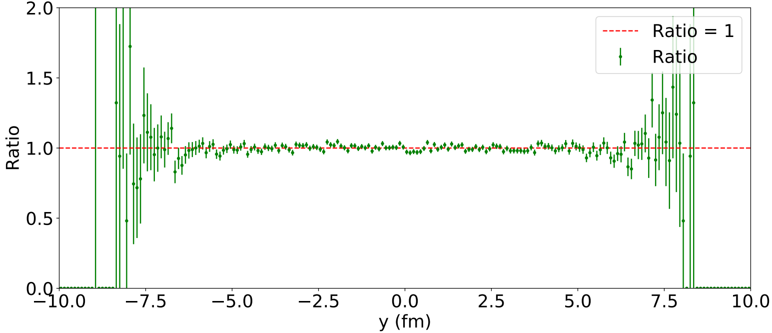

Figure 13: Ratio of the MC distribution cross section at $x = 0.05$ fm to the slice of the 2D collision density taken along y at $x = 0.05$ fm for the $Pb + Pb$ 0-5% centrality class at $\sqrt{s_{NN}} = 5.5$ TeV.

$$
\begin{aligned}
\frac{dp_i}{dt} &= -\mu p_i + F_i^L + F_i^T & (9)\\
< F_i^L(t_1)F_j^L(t_2) > &= \kappa_L \hat{p}_i \hat{p}_j g(t_2 - t_1), \quad \hat{p} = p_i/|\vec{p}| & (10)\\
< F_i^T(t_1)F_j^T(t_2) > &= \kappa_T(\delta_{ij} - \hat{p}_i \hat{p}_j) g(t_2 - t_1) & (11)\\
\kappa_T &= \pi\sqrt{\lambda}T^3\gamma^{1/2}, \quad \kappa_L = \gamma^2\kappa_T & (12)\\
\gamma &\lesssim \gamma_{lect}^{fluc} = \frac{M_Q^2}{4T^2} & (13)
\end{aligned}
$$

- Quark initial direction of propagation(assumed uniform) were randomly sampled
- Propagation was through backgrounds generated by the VISHNU2+1D hydrodynamics code
- Pseudo-random number generation was performed using the Ran routine from Numerical Recipes

EE and ET

- **ET parameters:**
  - 't Hooft coupling is taken to be $\lambda = 4\pi\alpha_s N_c = 4\pi \times 0.3 \times 3$ and $T_{QCD-plasma} = T_{SYM-plasma}$
- **EE parameters:**
  - 't Hooft coupling is taken to be $\lambda = 5.5$ and $T_{SYM-plasma} = T_{QCD-plasma}/3^{1/4}$
  - Can "experimentally measure" the strength of H.Q potential in lattice QCD (#/R) and compare to that calculated in AdS/CFT ($\sqrt{\lambda}/R$)
  - Can dial up/down $\sqrt{\lambda}$ to get a description like lattice QCD and that gives the λ=5.5
- In the EE prescription, the 't Hooft coupling is smaller by ≈ 2 and T is lower. So the drag for EE is smaller then we get less energy loss and less suppression

Heavy quarks position and momentum

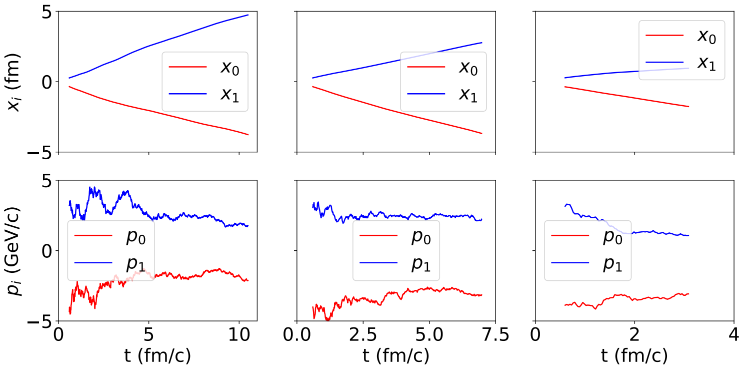

Figure 14: Position and Momentum of a single bottom quark produced at (0,0) fm with initial momentum (-4,3) GeV/c propagating through a VISHNU hydrodynamic background for different centralities as follows: 0-5% (Left), 30-40% (Middle) and 70-80% (Right).

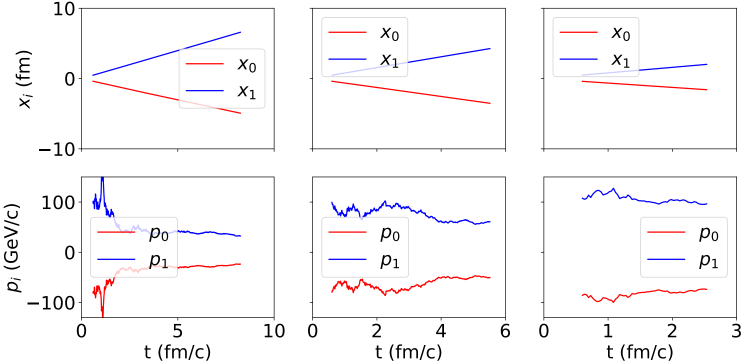

Figure 15: Position and Momentum of a bottom quark produced at (0,0) fm with initial momentum (-80,100) GeV/c propagating through a VISHNU hydrodynamic background for different centralities as follows: 0-5% (Left), 30-40% (Middle) and 70-80% (Right).

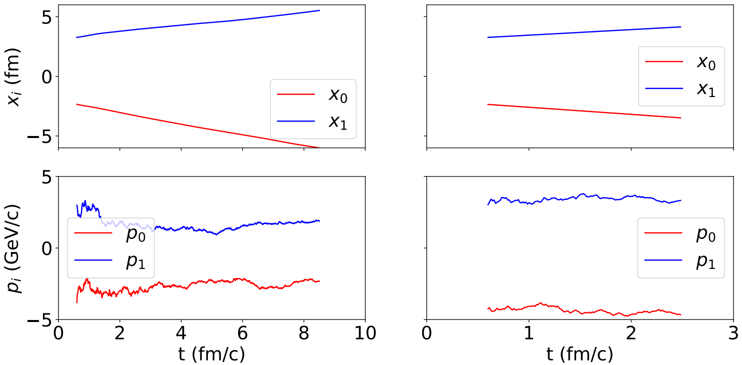

Figure 16: Position and Momentum of a single bottom quark produced at (-2,3) fm with initial momentum (-4,3) GeV/c propagating through a VISHNU hydrodynamic background for different centralities as follows: 0-5% (Left) and 30-40% (Right).

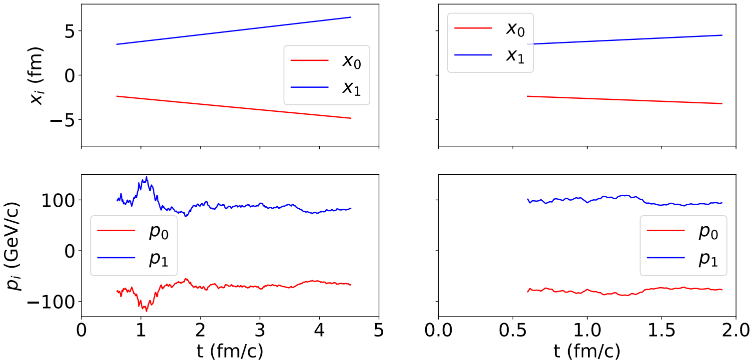

Figure 17: Position and Momentum of a single bottom quark produced at (-2,3) fm with initial momentum (-80,100) GeV/c propagating through a VISHNU hydrodynamic background for different centralities as follows: 0-5% (Left) and 30-40% (Right).

More $R_{AA}(p_T)$ results

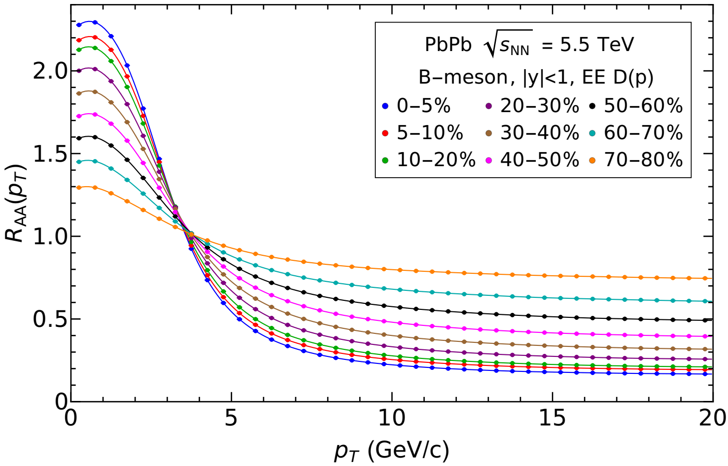

Figure 18: Expanded view of the transverse momentum region, $0 < p_T \leq 20$ GeV/c of Fig. (5a), including the region $R_{AA}(p_T) > 1$.

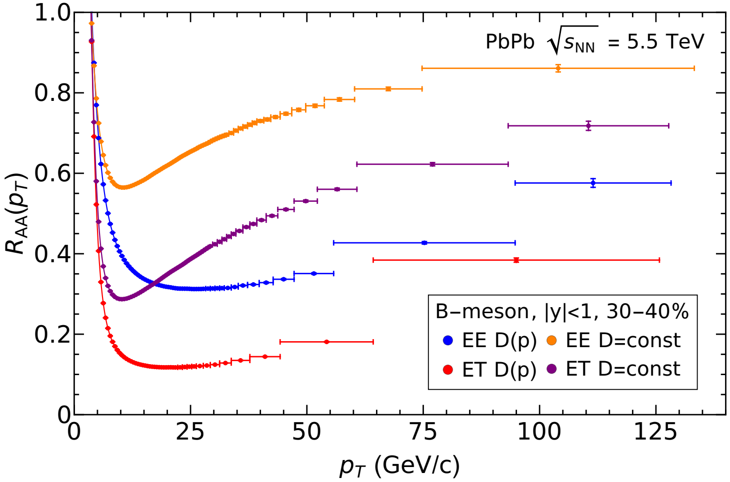

Figure 19: B-meson $R_{AA}(p_T)$ at $\sqrt{s_{NN}} = 5.5$ TeV for the 30-40% centrality class.

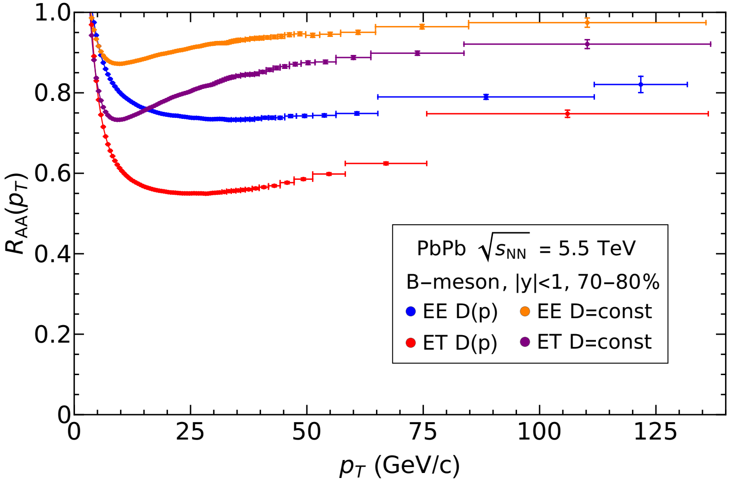

Figure 20: B-meson $R_{AA}(p_T)$ at $\sqrt{s_{NN}} = 5.5$ TeV for the 70-80% centrality class.

More $v_2(p_T)$ results

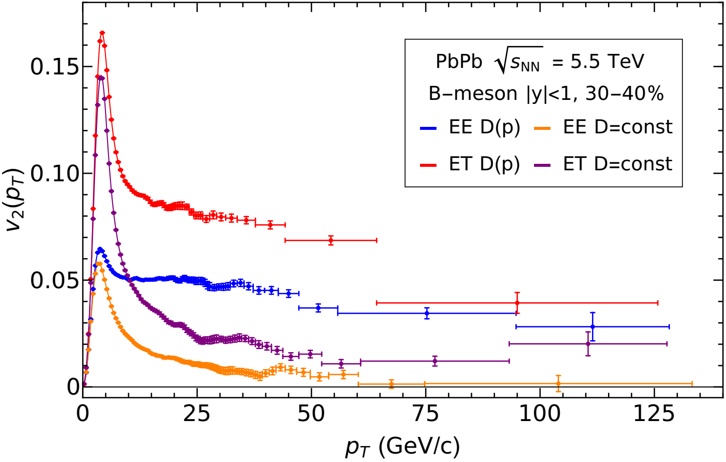

Figure 21: B-meson $v_2(p_T)$ at $\sqrt{s_{NN}} = 5.5$ TeV for the 30-40% centrality class.

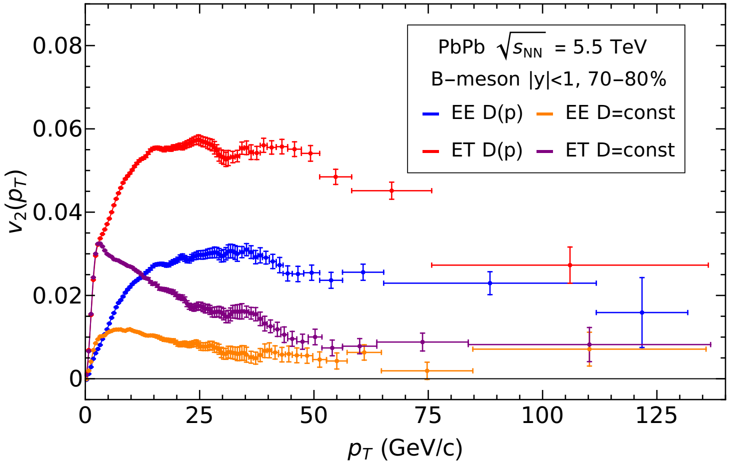

Figure 22: B-meson $v_2(p_T)$ at $\sqrt{s_{NN}} = 5.5$ TeV for the 70-80% centrality class.